Model-based polarimetric decomposition with higher-order statistics

Torbjørn Eltoft, *Member, IEEE* and Anthony P. Doulgeris, *Senior Member, IEEE*

***Abstract*—This paper presents a new general framework for solving polarimetric target decompositions that extends them to use more statistical information and include radar texture models. Polarimetric target decomposition methods generally have more physical parameters than equations, are thus underdetermined and have no unique solution. The common approach to solve them is to make certain assumptions, thus fixing some parameters, allowing the other parameters to be solved freely. This paper explains how to obtain additional equations from several statistical moments to find unique solutions and to address the issue of textured product models. The current work extends our previous conference works [1], [2], [3]. Preliminary results are demonstrated for a well known real polarimetric SAR scene for the 3-component Freeman-Durden decomposition.**

I. Introduction

THE backscatter of synthetic aperture radar (SAR) signals from many natural surfaces is often modelled as being caused by a combination of several scattering mechanisms, in general categorised as surface scattering, volume scattering, and double bounce scattering. An important research topic in SAR polarimetry focuses on the decomposition of the polarimetric SAR (polSAR) signals into components representing these mechanisms [4], [5]. The polarimetric decomposition theorems are generally categorised into to main categories; coherent methods, which devise strategies for decomposing the Sinclair matrix, and incoherent methods, which decompose the polarimetric covariance or coherence matrices. The former strategy addresses very high-resolution systems for which the scattering object is considered to be a pure target, whereas the latter describes distributed targets. Within the incoherent category, one approach is referred to as *model-based decompositions*, in which the measured covariance matrix is hypothesised as a combination of a number of individual matrices representing scattering as predicted by models. The Freeman-Durden Three-Component Model [6], the Four-Component Ymaguchi Model [7], and the Nonnegative Eigenvalue Decompositon Model [8] are three well-known examples of these types of decompositions. The parameters defining these model matrices are determined by solving a set of equations constructed by equating terms in the combination of model matrices with corresponding terms in the measured coherence (or covariance) matrix.

The authors are with the Department of Physics and Technology, UiT - The Arctic University of Norway, NO-9037 Tromsø, Norway (e-mail: {torborn.eltoft; anthony.p.doulgeris}@uit.no).

The research is funded by CIRFA partners and the Research Council of Norway (grant number 237906).

Digital Object Identifier XX.XXXX/GRSL.200X.XXXXXX

There are several weaknesses associated with the model-based decomposition models. One problem is that based on the covariance matrix alone it is not possible to construct enough equations to uniquely solve for the unknown parameters. The set of equations is underdetermined. This is usually solved by adding conditions which may or may not be valid, and implementing a sequential procedure for solving the parameters in which one scattering mechanism is extracted at a time. In addition, the first two of the above referred models may produce unphysical scattering mechanisms because they did not ensure that the resulting matrices in the decomposition individually represent realisable matrices. Van Zyl et al. [8] pointed out this problem, and proposed a simple check to ensure that the eigenvalues of the matrices of the individual scattering processes will be nonnegative. Lim et al. [9] explored further constrained optimisations, but still only on the second-order covariance matrices.

This paper addresses model-based decomposition in polSAR data by integrating additional statistical information to the parameter estimation problem. We show that going below and beyond second order statistics, we can construct additional equations, and hence ensure that the set of equations is determined. In addition, our example's empirical optimisation approach partly accounts for speckle variation during a cost function minimisation, and ensures physically valid solutions.

The paper is organised with Section II outlining the theoretical considerations for incoherent decomposition methods, the Freeman-Durden 3-component decomposition, and the extension of the statistical modelling to different moment orders. The example empirical optimisation approach is explained in Section II-C and the main features are demonstrated in Section III. Finally, we conclude in Section IV.

II. Theoretical considerations

A. Incoherent decomposition

The basic representation of the polarimetric scattering signal is by the so-called scattering feature vector. Under the reciprocity assumption this is 3-dimensional, and the lexicographic feature vector is defined as $\mathbf{k}_L = [S_{HH}, \sqrt{2}S_{HV}, S_{VV}]$.

The corresponding polarimetric covariance matrix is defined as $\mathbf{C} = E\{\mathbf{k}_L \mathbf{k}_L^\dagger\}$, where $E\{\cdot\}$ denotes statistical expectation. $\mathbf{C}$ is a nonnegative definite, Hermitian symmetric, 3×3 complex-valued matrix, with real-valued diagonal terms. In the remainder, we will use $\mathbf{k}$ (i.e. with subscript L suppressed) for the scattering vector.

The incoherent polarimetric decomposition strategy is to write this matrix as a superposition of contributions form several (N_s) scattering mechanisms, i.e.

$$\mathbf{C} = \sum_{i=1}^{N_s} P_i \tilde{\mathbf{C}}_i, \tag{1}$$

where $\tilde{\mathbf{C}}_i$ denotes the *span-normalised* covariance matrix of component i, and P_i represents the corresponding component power. Note that in [6], the authors normalise the VV-component. It hence follows that the span of $\mathbf{C}$, henceforth denoted $\mathcal{S}\{\mathbf{C}\}$, becomes the sum of powers P_i.

We will here adopt the same scattering component models as in the three-component Freeman-Durden (FD) decomposition [6] model, i.e. single-bounce, double-bounce, and volume scattering. As described in [6], the volume scattering component assumes the scattering particles to be a set of randomly oriented non-interacting thin dipoles, the single-bounce surface model is derived from a first order Bragg scattering, and the double-bounce model was derived from two Fresnel surface reflections. The span normalised covariance matrix formulation is given by

$$\tilde{\mathbf{C}}_s = \frac{1}{1+\beta^2}\begin{bmatrix} \beta^2 & 0 & \beta \\ 0 & 0 & 0 \\ \beta & 0 & 1 \end{bmatrix}, \tag{2}$$

$$\tilde{\mathbf{C}}_d = \frac{1}{1+|\alpha|^2}\begin{bmatrix} |\alpha|^2 & 0 & \alpha \\ 0 & 0 & 0 \\ \alpha^* & 0 & 1 \end{bmatrix}, \tag{3}$$

$$\tilde{\mathbf{C}}_v = \frac{3}{8}\begin{bmatrix} 1 & 0 & 1/3 \\ 0 & 2/3 & 0 \\ 1/3 & 0 & 1 \end{bmatrix}, \tag{4}$$

where α (complex) and β (real) are target specific parameters. Although this model is reflection symmetric, our modelling approach does not require this.

B. Statistical interpretation of the incoherent decompositions

Let us now consider a discrete statistical mixture model, i.e. a model where the random vector $\mathbf{k}$ has a probability density function (pdf) given as

$$p_{\mathbf{k}}(\mathbf{k}) = \sum_{i=1}^{N_s} f_i p_{\mathbf{k}_i}(\mathbf{k}). \tag{5}$$

Note that here the f_i's are generally interpreted as the a priori probability of an observation being generated by scattering mechanism i, and $\sum_{i=1}^{N_s} f_i = 1$. Assuming independence, the $\mathbf{C}$-matrix associated with the pdf of Eq.(5) becomes

$$\mathbf{C} = \int \mathbf{k}\mathbf{k}^\dagger p_{\mathbf{k}}(\mathbf{k}) d\mathbf{k} = \sum_{i=1}^{N_s} f_i \mathbf{C}_i, \tag{6}$$

where $\mathbf{C}_i$ is the covariance matrix of the individual mixture component i, including the component's power.

We note that the statistical mixture model leads to a similar second order moment equation as the incoherent decompositions, but involving the non-normalised component matrices. Hence, thinking about incoherent polarimetric decompositions as statistical mixing models leads to a probabilistic interpretation of the scattering process that may be carried all the way back to the scattering feature vector level $\mathbf{k}$. As will be shown in the next section, this interpretation opens the possibility to increase the number of parameter equations, such that the equation set becomes determined. It follows from (6) that the total span of $\mathbf{C}$ is given as $\mathcal{S}\{\mathbf{C}\} = \sum_{i=1}^{N_s} f_i \mathcal{S}\{\mathbf{C}_i\}$. Comparing with the traditional Freeman-Durden, we can conclude that the statistical mixture fraction is related to the power fraction through the relation $f_i = P_i/\mathcal{S}(\mathbf{C}_i)$, that is, the fraction (ratio) of the pure component power being mixed rather than the fraction (amount) of VV power as in [6].

C. Statistcal modelling

In what follows, we will expand on the implications of interpreting incoherent polarimetric decompositions as a statistical mixture model. It is commonly assumed that the scattering vector is Gaussian distributed. A Gaussian scattering feature vector is presumed to have a circular symmetric complex Gaussian pdf, which is completely determined by its second-order moment. The d-dimensional probability density function of a complex circular symmetric Gaussian scattering feature vector, $\mathbf{k}$, is given as:

$$p_{\mathbf{k}}(\mathbf{k}) = \frac{1}{\pi^d |\mathbf{C}|} \exp(-\mathbf{k}^\dagger \mathbf{C}^{-1} \mathbf{k}), \tag{7}$$

where, as before, $\mathbf{C} = \mathrm{E}\{\mathbf{k}\mathbf{k}^\dagger\}$ is the covariance matrix of $\mathbf{k}$.

However, many studies have shown that the Gaussian assumption is not always true [10], [11], [12], especially when the data is collected by high-resolution polSAR radar systems. Non-Gaussianity may be caused by two few scatterers per resolution cell causing non fully developed speckle interference, or due to local variation of physical class properties. In these cases, the statistics may deviate significantly from the Gaussian model. The mixture model presented in (5) is in general not a Gaussian model, even if the individual components are Gaussian, meaning that also moments of the total scattering feature vector below and beyond second order may add information about the scattering process.

In recent years, it has been shown by several authors that the so-called *product model* represents a simple and valid statistical description for non-Gaussian polarimetric data [13], [14], [15], [16]. In the following, we will also assume that the individual components deviate from Gaussian statistics, and that they can be modelled by the product model. The product model presumes that the observed variation in SAR backscatter is composed of two independent components, one describing natural variation in the mean reflectivity, called texture, and another for Gaussian speckle [13]. Using this formulation, we can write the feature vector of a scattering mechanism, i, as

$$\mathbf{k}_i = \sqrt{\tau_i}\mathbf{C}_i^{\frac{1}{2}}\mathbf{n}, \tag{8}$$

where the scale parameter for texture τ_i is a strictly positive scalar random variable, normalised such that its mean $\mathrm{E}\{\tau_i\} = 1$, and $\mathbf{n}$ is a standardised, complex multivariate

Gaussian vector, independent of τ_i, with zero mean and identity covariance matrix, i.e. $\mathbf{n} \sim \mathcal{N}^c(\mathbf{0}, \mathbf{I})$. Each dimension of $\mathbf{n}$ is a one-dimensional circular symmetric complex Gaussian random variable.

We will now briefly examine the component-wise distributions for scattering feature vector $\mathbf{k}_i$, $i = 1, 2, \cdots, N_s$, i.e. the scattering vector associated with scattering mechanism i. For dimension component j, we may write $k_{j,i} = \mathcal{R}(k_{j,i}) + j\mathcal{I}(k_{j,i})$, where $\mathcal{R}(\cdot)$ and $\mathcal{I}(\cdot)$ refer to real and imaginary parts, respectively. We note that, for a given τ_i, $k_{j,i}$ of (8) is a circular symmetric complex Gaussian random variable, implying that $\mathcal{R}(k)$ and $\mathcal{I}(k)$ are are statistically independent and identically distributed (iid) with zero mean, and their joint pdf becomes

$$p(\mathcal{R}(k_{j,i}), \mathcal{I}(k_{j,i})|\tau_i) = \frac{1}{\pi\tau_i C_{jj,i}} \exp\left(-\frac{\mathcal{R}(k_{j,i})^2 + \mathcal{I}(k_{j,i})^2}{\tau_i C_{jj,i}}\right). \tag{9}$$

It is furthermore easy to validate that the amplitude $|k_{j,i}| = \sqrt{\mathcal{R}(k_{j,i})^2 + \mathcal{I}(k_{j,i})^2}$, conditioned on τ_i, follows a Rayleigh distribution, given as

$$p(|(k_{j,i})|\,|\tau_i) = \frac{2|k_{j,i}|}{\pi\tau_i C_{jj,i}} \exp\left(-\frac{|k_{j,i}|^2}{\tau_i C_{jj,i}}\right). \tag{10}$$

The moment of order l of $|k_{j,i}|$ of can hence be expressed as

$$\mathrm{E}\{|k_{j,i}|^l\} = E\{\tau_i^{\frac{l}{2}}\} C_{jj,i}^{\frac{l}{2}}\, \Gamma(1 + \frac{l}{2}). \tag{11}$$

Applying (11) to the mixture model in (6), we readily see that we may write

$$\mathrm{E}\{|k_j|^l\} = \sum_{i=1}^{N_s} f_i E\{\tau_i^{\frac{l}{2}}\} C_{jj,i}^{\frac{l}{2}}\, \Gamma(1 + \frac{l}{2}), \tag{12}$$

where k_j refers to the j^{th} dimension of the measured $\mathbf{k}$.

This theory may be used to formulate d marginal equations, $j = 1 \ldots d$, for each order l. These expressions are in terms of the diagonal elements of $\mathbf{C}_i$, but are unique and non-linear due to the mixing fractions and the order. However, introducing texture has also introduced an additional texture parameter (or two) for each component, so, excepting for simplified cases, several orders may need to be combined to obtain sufficient equations for a unique solution. A texture distribution model will be needed to link the different orders and avoid over-many texture parameters.

sectionEmpirical Optimisation

In [1], [2], [3] we introduced the optimisation concept for simplified models with only one higher order and either no texture (Gaussian) or only one texture parameter for all components. Here, we will continue and demonstrate that using multiple moments allows solving for different component textures.

We take the case of the three component Freeman-Durden decomposition detailed in Section II, for which the second order covariance matrix gives five real valued equations (three diagonals plus a real and imaginary off diagonal) for its six real parameters $f_s', f_d', f_v', \beta_{\text{real}}, \alpha_{\text{real}}, \alpha_{\text{imag}}\}$. We note that these are power fractions in the original Freeman-Durden formulation, and not the same as the mixing fractions that we need to interpret, so we must introduce three new parameters for mixing component powers (in terms of span $\{S_s, S_d, S_v\}$), and we wish to account for three texture terms, one for each component. The texture will be introduced as a parameter to a model such as the K or G^0 distributions such that we can connect to different moment orders. This gives a total of 12 free parameters and hence we need to find at least seven new equations over the 5 from the second order. We have one equation from the constraint that the mixing fractions sum to one and, following our previous works, we can obtain an equation for each diagonal moment order and for each polarimetric dimension. By combining moment orders 1, 3, and 4 for each of HH, HV, and VV channels, we obtain 9 new equations, which is sufficient.

We suggest that this scenario should not only find a unique solution, but the over determined system of equations and minimising the error also allows for some degree of remnant speckle variation in the multi-looked data values. Such variation is not always accounted for in target decomposition solutions. In addition, the forward modelling construction will always guarantee physically valid, and non-negative eigenvalue, solutions, so long as we make sure to apply non-negative limits on the mixing fractions and physically valid ranges on other parameters.

As before, we construct a total error (sum of squared errors) cost function from the difference between the observed moment for each term (equation) and the model prediction given the parameters, and then optimise this by searching over the parameter space (forward modelling search). As before, we discussed that the scale of each term could lead to a dominance of the total error by the biggest terms, and hence we have normalised each error term by its observed variance in an attempt to balance the influence of each expression. We measure the observed variance for each term in a pre-processing scan with a 3×3 window. In addition, we applied some empirically determined transformations, to both the observations and the model terms, to improve the distribution symmetry towards the Gaussian to apply such a simple concept of variance normalised errors. Each marginal moment uses the n^{th} root, including the second order from the covariance matrix diagonals, and the off diagonal real and imaginary parts are taken as they are.

The final cost function optimisation can be formulated as

$$\begin{aligned}
\underset{\Theta}{\arg\min} \;=\; & \sum_{p=1}^{3}\sum_{m=1}^{4} \frac{\left(\sqrt[m]{\mathrm{E}\{|k_p|^m\}} - \sqrt[m]{\langle|k_p|^m\rangle}\right)^2}{\mathrm{var}\{\sqrt[m]{\langle|k_p|^m\rangle}\}} \\
& + \frac{\left(\mathrm{E}\{\mathcal{R}(C_{1,3})\} - \langle\mathcal{R}(C_{1,3})\rangle\right)^2}{\mathrm{var}\{\langle\mathcal{R}(C_{1,3})\rangle\}} \\
& + \frac{\left(\mathrm{E}\{\mathcal{I}(C_{1,3})\} - \langle\mathcal{I}(C_{1,3})\rangle\right)^2}{\mathrm{var}\{\langle\mathcal{I}(C_{1,3})\rangle\}}
\end{aligned} \tag{13}$$

where $\Theta = \{f_s', f_d', f_v', S_s, S_d, S_v, \beta_{\text{real}}, \alpha_{\text{real}}, \alpha_{\text{imag}}, \tau_s, \tau_d, \tau_v\}$, we have p polarimetric dimensions plus m moment orders plus the real and imaginary off-diagonal terms, and $\mathrm{E}\{\cdot\}$ from (11) is expected from the parametric model and $\langle\cdot\rangle$ is from the transformed observation. We used an optimisation toolbox function `fmincon()` in MatLab to solve this set

of constrained equations, including the fractions summing to one condition and limits on the parameters, and applied it to each pixel individually. This approach is quite slow and takes several hours to process this small scene, however, it demonstrates that a solution is possible and should be easy to apply it to parallel processing in the future.

III. Results

Having chosen to demonstrate the well known Freeman-Durden decomposition, we similarly chose the San Francisco city scene because it is quite familiar to the polarimetric SAR community and has been used in many papers and textbooks. The result is using a sample RADARSAT-2 quad-pol scene and has been processed to 10×5 looks. We shall compare our method to the standard Freeman-Durden decomposition solution, although non-negative eigenvalue solutions also exist.

We shall demonstrate that our solution produces visually similar component powers via the RGB representation, we produce complete parameter solutions (without needing to fix any terms under certain conditions), and we produce additional information such as the texture.

The Freeman-Durden powers can be plotted as Red: $P_d =$ SPAN $\times$ f'_d, Green: $P_v =$ SPAN $\times$ f'_v, and Blue: $P_s =$ SPAN $\times$ f'_s. In our modelling, with the slightly different interpretation of the fractions, we multiply by their individual component spans. Figure 1 shows the traditional Freeman-Durden RGB image and Figure 2 shows our optimisation results. Note that our solution produces less green coloured volume scattering in some areas, which was a known failing of the original Freeman-Durden solution.

The real valued β parameter for the surface scattering strength is displayed in Figure 3 and 4. To obtain a solution from the under-determined set of equations, the traditional approach had to fix the least important parameter to solve for the remainder. This means that the surface β parameter is set to +1 where double-bounce is dominant in the urban areas, whereas our solution for this parameter is often quite different from this assumed value and appears a lot more blue. There is a similar behaviour for the double-bounce alpha parameter (not shown), although it is a lot noisier to interpret due to the textural variation in the urban areas. A recent study in [17] has demonstrated that this simple fixed constraint severely biases the resulting solution.

The final demonstration is the extra information obtained as the texture parameter. Figure 5 shows a representation of the texture parameter for the surface component that clearly indicates lower texture over the ocean and higher in the urban areas as would be expected.

In all figures we see that there is significant noise, particularly over the ocean area, and this was not expected. We had anticipated that some of the speckle variation would be absorbed due to the minimisation approach rather than the analytical solution from equations assuming no error. We believe that this may be due to our equal weighting for all equations and terms, even though the normalisation to variance was intended to balance the equation set. We need to explore this further and determine whether some terms may have more combined variation than others and may need uneven weighting, or alternatively find another balanced cost mechanism.

IV. Conclusions

We conclude by claiming that we have demonstrated a novel strategy to generically add extra equations to uniquely solve traditionally under-determined target decomposition schemes. We have demonstrated that the well known Freeman-Durden three component model can be solved in this way and that the power components look similar and realistic, that the internal parameters are estimated everywhere without making assumptions, and that we obtain extra parametric information such as texture. The approach is currently slow and noisy, but we have only attempted to demonstrate the feasibility of obtaining extra equations for the solution.

The higher-order moment approach is generic for any equation set, although it does add several additional free parameters and required some empirical variance estimates

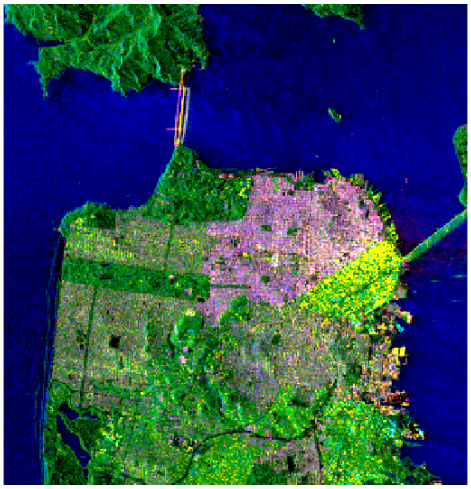

Fig. 1. Traditional Freeman-Durden solution as power RGB image.

Fig. 2. Our numerically optimised solution as power RGB image.

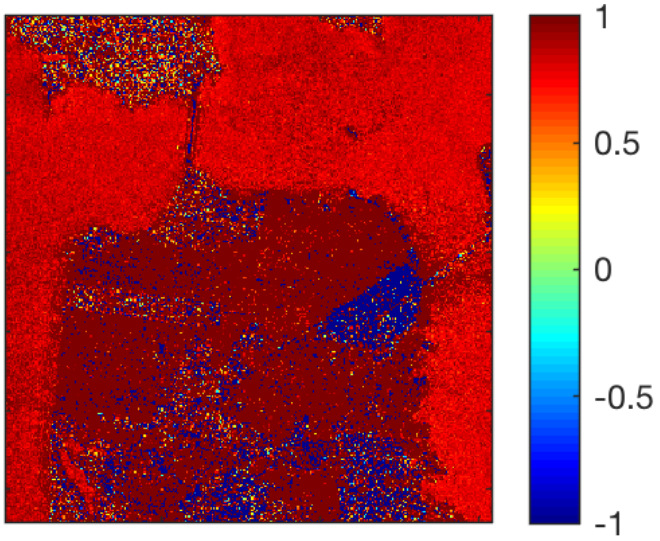

Fig. 3. Traditional Freeman-Durden surface β parameter image. Urban areas were explicitly set to +1 to solve the otherwise under-determined system.

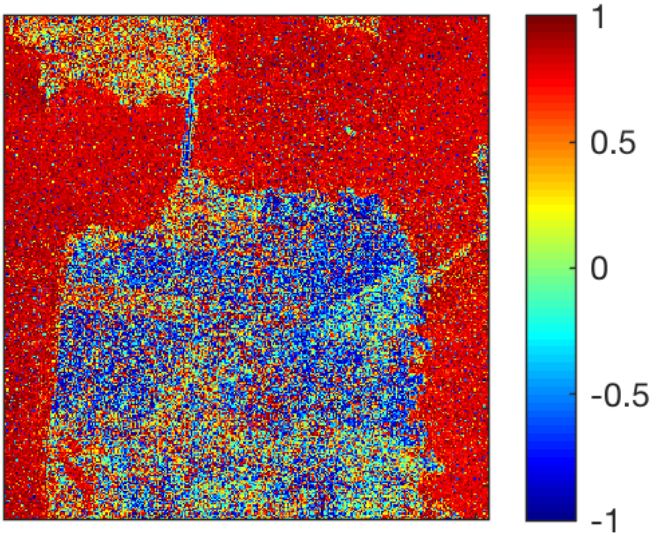

Fig. 4. Our numerically optimised solution for the surface β parameter is complete over all pixels, although we note significant noise everywhere.

in its current form. It is hoped that further research may determine theoretical variance expressions and find a better weighted cost function for optimisation.

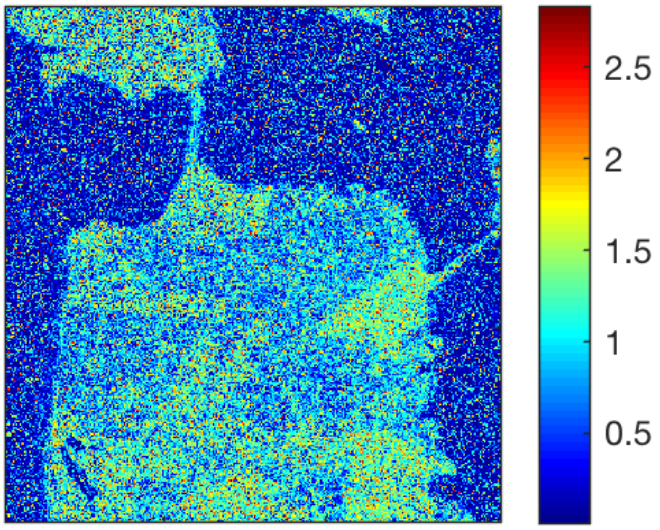

Fig. 5. An example of a texture parameter. Low values (dark blue) indicate homogeneous areas, while high values (yellow to red) indicate radar texture.

REFERENCES

[1] A. P. Doulgeris and T. Eltoft, "Can higher-order statistics add information in model-based polarimetric decompositions?" in *proc. PolinSAR 2015*, Frascati, Italy, January 26-30 2015.

[2] A. Doulgeris and T. Eltoft, "Aspects of model-based decompositions in radar polarimetry," in *proc. IGARSS 2015*, Milan, Italy, July 26-31 2015.

[3] A. P. Doulgeris and T. Eltoft, "An empirical optimisation strategy for model-based polarimetric target decomposition," in *11th European Conference on Synthetic Aperture Radar (EUSAR2016)*, June 6–9, Hamburg, Germany 2016.

[4] J.-S. Lee and E. Pottier, *Polarimetric Radar Imaging: From Basics to Applications*, ser. Optical Science and Engineering. Boca Raton, USA: CRC Press, 2009, no. 143.

[5] J. J. van Zyl and Y. Kim, *Synthetic Aperture Radar Polarimetry*. Wyley & Sons, US: John Wiley & Sons, Inc, 2011.

[6] A. Freeman and S. L. Durden, "A three-component scattering model for polarimetric SAR data," *IEEE Trans. Geosci. Remote Sens*, vol. 36, no. 3, pp. 963–973, May 1998.

[7] Y. Yamaguchi, T. Moriyama, M. Ishido, and H. Yamada, "Four-component scattering model for polarimetric SAR image decomposition," *IEEE Trans. Geosci. Remote Sens.*, vol. 43, no. 8, pp. 1699–1706, Aug. 2005.

[8] J. J. van Zyl, M. Arii, and Y. Kim, "Model-based decomposition of polarimetric sar covariance matrices constrained for non-negative eigenvalues," *IEEE Trans. Geosci. Remote Sens.*, vol. 49, no. 8, pp. 2251–2258, Aug. 2011.

[9] Y. X. Lim, M. S. Burgin, and J. J. van Zyl, "An optimal nonnegative eigenvalue decomposition for the freeman and durden three-component scattering model," *IEEE Transactions on Geoscience and Remote Sensing*, vol. 55, no. 4, pp. 2167–2176, April 2017.

[10] A. P. Doulgeris, S. N. Anfinsen, and T. Eltoft, "Classification with a non-Gaussian model for PolSAR data," *IEEE Trans. Geosci. Remote Sens.*, vol. 46, no. 10, pp. 2999–3009, Oct. 2008.

[11] A. P. Doulgeris and T. Eltoft, "Scale mixture of Gaussian modelling of polarimetic SAR data," *Eurasip J. Adv. Sig. Proc.*, vol. 2010, 12 pp., Jan. 2010.

[12] G. Vasile, J.-P. Ovarlez, and F. Pascal, "Estimation and segmentation in non-Gaussian POLSAR clutter by SIRV stochastic processes," in *Proc. IEEE Int. Geosci. Remote Sens. Symp., IGARSS 2009*, vol. 3, Cape Town, South Africa, 12-17 July 2009, pp. 963–966.

[13] C. Oliver and S. Quegan, *Understanding Synthetic Aperture Radar Images*, 2nd ed. Raleigh, USA: SciTech Publishing, 2004.

[14] T. Eltoft, S. Anfinsen, and A. Doulgeris, "A multitexture model for multilook polarimetric synthetic aperture radar data," *IEEE Trans. Geosci. Remote Sens.*, vol. 52, no. 5, pp. 2910–2919, May 2014.

[15] A. P. Doulgeris, S. N. Anfinsen, and T. Eltoft, "Automated non-Gaussian clustering of polarimetric synthetic aperture radar images," *IEEE Trans. Geosci. Remote Sens.*, vol. 49, no. 10, pp. 3665–3676, Oct. 2011.

[16] G. Vasile, E. Trouvé, J.-S. Lee, and V. Buzuloiu, "Intensity-driven adaptive-neighborhood technique for polarimetric and interferometric SAR parameters estimation," *IEEE Trans. Geosci. Remote Sens.*, vol. 44, no. 6, pp. 1609–1621, Jun. 2006.

[17] T. L. Ainsworth, J.-S. Lee, and Y. Wang, "Model-based polsar decompositions: Virtues and vices," in *2018 IEEE International Geoscience and Remote Sensing Symposium (IGARSS)*, 2018.